First measurements of g factors in the even Kr isotopes

T. J. Mertzimekis,[1] N. Benczer-Koller,[1] J. Holden,[1] G. Jakob,[1] G. Kumbartzki,[1] K.-H. Speidel,[2] R. Ernst,[2] A. Macchiavelli,[3] M. McMahan,[3] L. Phair,[3] P. Maier-Komor,[4] A. Pakou,[5] S. Vincent,[6] and W. Korten[7]

[1]*Department of Physics and Astronomy, Rutgers University, New Brunswick, New Jersey 08903*

[2]*Institut für Strahlen- und Kernphysik, Universität Bonn, D-53115 Bonn, Germany*

[3]*Lawrence Berkeley National Laboratory, Berkeley, California 94720*

[4]*Technische Universität München, D-85748 Garching, Germany*

[5]*Department of Physics, The University of Ioannina, GR-451 10 Ioannina, Greece*

[6]*Department of Physics, University of Notre Dame, South Bend, Indiana 46556*

[7]*CEA Saclay, DAPNIA/SPhN, Gif-sur-Yvette F-91191, France*

(Received 30 March 2001; published 17 July 2001)

The g factors of the 2_1^+ and 4_1^+ states in ^{78,80,82,84,86}Kr have been measured for the first time, using Coulomb excitation of isotopic Kr beams and the transient field technique. The measured g factors of 2_1^+ states in ^{78,80,82}Kr are well described, in both magnitude and progression with neutron number, by the IBA-II model. Whereas the lighter isotopes show a dominant collective structure with g factor values close to Z/A, the large $g(2_1^+)=1.12(14)$ value of ^{86}Kr, with its closed $N=50$ shell, is unequivocally dominated by specific proton configurations. The g factor of the 2_1^+ state in ^{84}Kr, with two holes in the $1g_{9/2}$ neutron orbit, reflects both proton and neutron components in the wave function. In addition, the lifetimes of several 2_1^+ and 4_1^+ states were remeasured by the Doppler shift attenuation method, yielding values which, in some cases, differ from those in the literature.

DOI: 10.1103/PhysRevC.64.024314 PACS number(s): 21.10.Ky, 25.70.De, 27.60.+j

I. INTRODUCTION

Kr nuclei ($Z=36$), lying between well-studied Se ($Z=34$) and Sr ($Z=38$) isotopes, represent a rich laboratory in which nuclear structure effects can be examined. The radioactive even ^{72}Kr, ^{74}Kr, and ^{76}Kr belong to the class of nuclei with $N\sim Z$, where both neutrons and protons occupy the same orbitals and which are characterized by strong neutron-proton pairing correlations [1]. These nuclei, together with the lighter stable isotopes ^{78}Kr, ^{80}Kr, and ^{82}Kr, exhibit collective structures with coexistent prolate and oblate shapes [2]. As the $N=50$ shell closure is approached for ^{84}Kr and ^{86}Kr, single-particle degrees of freedom of both protons and neutrons play the dominant role. In particular, particle-hole states in the fp shell ($2p_{3/2}$, $1f_{5/2}$, and $2p_{1/2}$), as well as the $1g_{9/2}$ orbital for protons and $1g_{9/2}$ hole states for neutrons, are expected to be the main components of the nuclear wave functions. A similar scenario of proton and neutron configurations was considered in the discussion of the experimental g factors of ^{86}Sr, ^{88}Sr [3], and ^{90}Zr [4]. Moreover, the proximity to Se isotopes, for which the precise g factors of the 2_1^+ states were well described by an IBA-II calculation [5], with an assumed closed neutron shell at $N=38$, raises the intriguing question as to whether this subshell closure may also exist for Kr isotopes. A systematic study of magnetic moments for the Kr isotopes as a function of the neutron number may clarify the many facets of the structure of isotopes in this region.

These are the first measurements of g factors for the excited 2_1^+ and 4_1^+ states of stable even Kr isotopes and include several new lifetimes. As Kr targets are difficult to prepare and are unstable under heavy ion beams, only with the combined techniques of projectile Coulomb excitation and transient hyperfine magnetic fields [5], in which Kr beams are excited by a light target nucleus, does it become feasible to measure magnetic moments. In inverse kinematics, both projectile and target ions are focused in the beam direction and are produced with high velocities, conditions favorable to simultaneous measurements of the spin precessions in the transient field and of the lifetimes of the nuclear states via the Doppler shift attenuation method (DSAM). These advantages were exploited in several previous measurements on other nuclei, yielding high-precision g factors and lifetimes. Details of the technique were described in various publications [4,5,7,8]. Distinguishing characteristics, pertaining to the current experiments and the extension of the analysis to the more general case, are presented below. Partial energy-level schemes [9–13] of the isotopes studied, showing mainly the transitions observed in the present measurements, are shown in Fig. 1.

II. EXPERIMENTAL TECHNIQUE

Isotopic beams of ^{78,80,82,84,86}Kr were accelerated at the Lawrence Berkeley National Laboratory 88 Inch Cyclotron, to energies between 220 and 261 MeV, with intensities of ~ 1 pnA. A single multilayer target was used for all isotopes. This target consisted of 0.9 mg/cm^2 of enriched ^{26}Mg evaporated on a 4.0 mg/cm^2 gadolinium layer, itself deposited on a 1.1 mg/cm^2 tantalum foil, backed by a 3.9 mg/cm^2 copper layer. The preparation of the ferromagnetic gadolinium foil was described in Ref. [14]. The isotope ^{26}Mg was selected as a suitable target because the excitation cross sections for the Kr nuclei are sufficiently large and γ-ray lines from target excitation do not contribute interfering background to the spectra. The kinematics applying to the various beams with the target were derived from the stop-

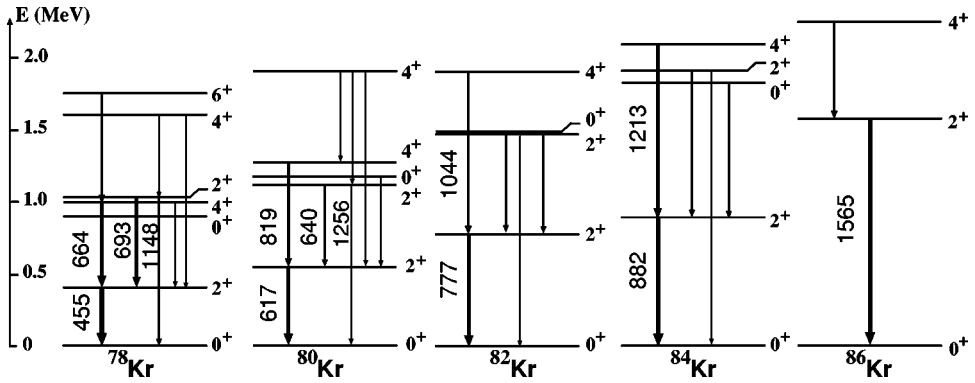

FIG. 1. Partial energy-level scheme of the low-energy states of the even Kr isotopes. The transitions used for the precession measurements are identified by their energy in keV.

ping powers of Ref. [15], and are shown in Table I.

The target was kept at ~77 K by a liquid-nitrogen reservoir. The gadolinium layer was magnetized by an external magnetic field of 0.06 T applied perpendicular to the γ-ray detection plane. The field direction was reversed every 3 min. The target magnetization was measured before and after the experiment and found to be constant, $M(77K) = 0.1872$ T.

The Kr ions that were Coulomb excited in the Mg layer were exposed to the transient magnetic field in the gadolinium layer before stopping in the copper backing. The beam itself was stopped in an additional 5.6 mg/cm^2 copper foil placed behind the target. The recoiling Mg ions traversed the whole target plus the beam stopper foil, and were detected in a 1.5×1.5 cm^2 solar cell particle detector placed at 0° with respect to the beam and masked by a circular aperture subtending an angle of 17°.

The γ rays were detected in coincidence with the forward-scattered Mg ions in either four NaI(Tl) (12.7×12.7 cm^2) or Ge (two of which had 40% and two 50% efficiency) detectors. The scintillators were used for ^{82,84,86}Kr because of their high photopeak efficiency. Ge detectors were essential for the measurements of the lighter isotopes ^{78,80}Kr, where higher resolution is required. ^{84}Kr was also measured with Ge detectors. The four γ-ray detectors were placed at $\pm68°$ and $\pm112°$ with respect to the beam direction for the precession measurements. An additional Ge detector (efficiency 25%), placed at 0° with respect to the beam, was used for lifetime measurements. Particle-γ angular correlations $W(\theta_\gamma)$ were determined from anisotropy measurements based on ratios of counting rates in pairs of detectors located alternately at angles θ_γ of $\pm50°$, $\pm130°$, $\pm80°$, and $\pm110°$. The advantage of this procedure, compared to carrying out a complete angular correlation measurement, is that these ratios are independent of counter-efficiencies and beam-related effects, thus reducing systematic errors. Typical spectra of γ rays detected in coincidence with the Mg ions are shown in Fig. 2.

TABLE I. Summary of reaction kinematics characteristics. $\langle E\rangle_{in}$, $\langle E\rangle_{out}$, $\langle v/v_o\rangle_{in}$, and $\langle v/v_o\rangle_{out}$ are the average energies (in MeV) and velocities (in units of the Bohr velocity, $v_o=e^2/\hbar$), of the ^{A}Kr isotopes entering into and exiting from the gadolinium foil, respectively. Δt (in ps) is the time the Kr ions spend in the ferromagnetic foil.

	E_{beam}	$\langle E\rangle_{in}$	$\langle E\rangle_{out}$	$\langle v/v_o\rangle_{in}$	$\langle v/v_o\rangle_{out}$	Δt
^{78}Kr	220.5	40.5	5.3	4.6	1.6	0.85
^{80}Kr	246.7	49.3	8.4	5.0	2.1	0.72
^{82}Kr	240.7	49.5	8.8	4.9	2.1	0.73
^{84}Kr	235.0	49.7	9.1	4.9	2.1	0.72
^{86}Kr	261.1	49.4	9.3	4.8	2.1	0.73

III. DATA ANALYSIS AND RESULTS

In general, if only one state is excited, the precession of the magnetic moment of that state is related to the effect ϵ

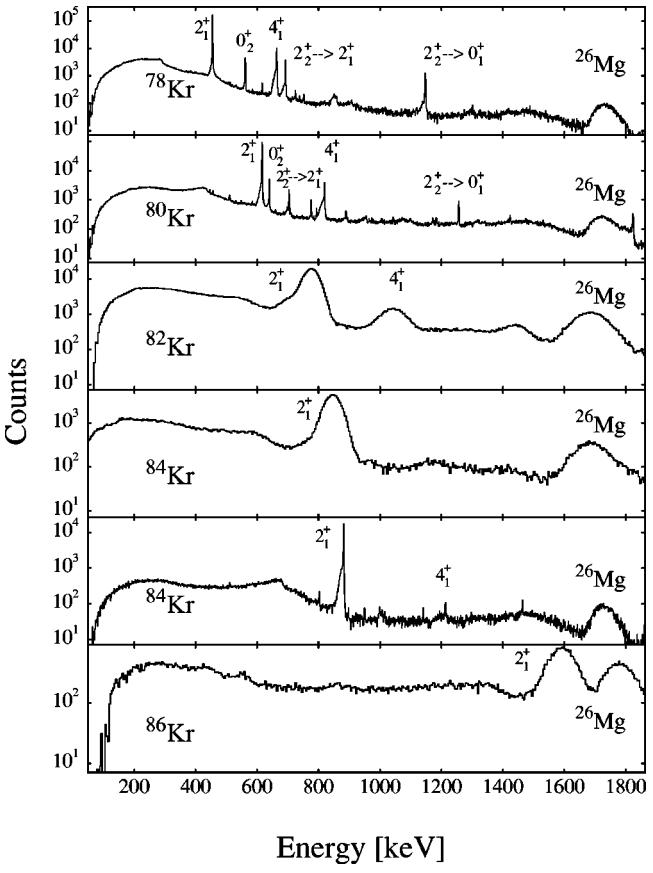

FIG. 2. Typical coincidence spectra obtained with Ge and NaI detectors. The high-energy peaks correspond to γ rays from the 2_1^+ state of Coulomb-excited ^{26}Mg in the target.

which is determined from the coincidence counting rates $N^{\uparrow}_{i,j}$ and $N^{\downarrow}_{i,j}$ of the photopeak of the γ transition in the ith or jth detector with the external field pointing "up" ($\uparrow$) or "down" ($\downarrow$) with respect to the γ-ray detection plane [5,7,8,16,17]. The effect ϵ is given by $\epsilon=(\rho-1)/(\rho+1)$, where $\rho=(\rho_{14}/\rho_{23})^{1/2}$ and $\rho_{ij}=[(N^{\uparrow}_i/N^{\downarrow}_i)/(N^{\uparrow}_j/N^{\downarrow}_j)]^{1/2}$.

The precession angle is then given by $\Delta\theta=\epsilon/S$, where

$$S(\theta_\gamma)=\frac{1}{W(\theta_\gamma)}\cdot\frac{dW(\theta)}{d\theta}\bigg|_{\theta=\theta_\gamma}$$

is the logarithmic slope of the angular correlation at the γ-ray detector angles. The logarithmic slope can be determined either from a direct measurement of the angular correlation $W(\theta_\gamma)$, or from measurements of an "anisotropy ratio" of intensities at two angles. In the present experiment, this "anisotropy ratio" R is given by

$$R(1/4)=\left(\frac{N_1(130°)N_4(-130°)}{N_1(100°)N_4(-100°)}\right)^{1/2}$$

and

$$R(2/3)=\left(\frac{N_2(50°)N_3(-50°)}{N_2(80°)N_3(-80°)}\right)^{1/2},$$

where $N_{i,j}(\theta_\gamma)\approx W_{i,j}(\theta_\gamma)$ are the coincidence photopeak intensities of the transition of interest in detectors i or j located at the indicated angles.

In order to derive the particle-γ angular correlation function

$$W^{expt}(\theta_\gamma)=1+\sum_k A^{expt}_k P_k(\cos\theta_\gamma) \tag{3.1}$$

from the measured R, the experimental correlation coefficients, A^{expt}_k must be determined. These coefficients can be written in terms of $A^{theo}_{2,4}$, the coefficients for the ideal case pertaining to the situation of a completely aligned system and two attenuation coefficients, Q_k, which corrects for the finite size of the Ge or NaI(Tl) detectors; and G_k, which accounts for the attenuation caused by the finite angle subtended by the particle detector $A^{expt}_k=G_kQ_kA^{theo}_k$. If the angle subtended by the particle detector is small, $G_k=1-Qk(k+1)$ [17]. Consequently, Q is the only parameter that needs to be determined to obtain the angular correlation coefficients A^{expt}_k and, therefore the logarithmic slope S. The measurement of the anisotropy ratio R is thus sufficient to determine S. In this experiment, R is measured for two sets of redundant angles, forward and backward, and the data are averaged to obtain the final result.

If the state of interest, say state q, is also fed from precursor higher-energy states, the analysis of the precession effect requires a more complex formulation. Elements of the analysis were presented in Refs. [5,17,18], but further details are added here for completeness in treating the general case. Since the lifetimes of the nuclear states are usually longer than the transit time through the ferromagnetic foil, the magnetic moments of all precursor states are the ones that precess in the hyperfine transient field as well as the moment of the state of interest, q. The measured precession effect corresponds to a weighted average of all precessions,

$$\langle\epsilon\rangle=\frac{\sum_m P_mB_mW_m\epsilon_m}{\sum_m P_mB_mW_m}, \tag{3.2}$$

where the index m runs from that of state q to all higher-energy states that decay to q. P_m is the Coulomb excitation probability of the mth state, B_m is the branching ratio for the cascade decay that ends up in state q, W_m is the angular correlation function for the decay of state q when excited through the decay of state m with the intervening radiations not observed, and the ϵ_m's are individual precession effects for each of the initial states m. A similar expression was derived and used by Stuchbery *et al.* [18].

The actual precession angle of the state q, which is populated directly, is given by $\Delta\theta_q=\epsilon_q/S_q$ and ϵ_q and can be extracted from the following equation:

$$\epsilon_q=\frac{\langle\epsilon\rangle\sum_m P_mB_mW_m-\sum_n P_nB_nW_n\epsilon_n}{P_qB_qW_q}. \tag{3.3}$$

The index n runs through all values of m, except $m=q$. The Coulomb excitation probabilities P_m, and branching ratios

TABLE II. Summary of the anisotropy ratios $\langle R\rangle$ measured at angles of 50°, 80°, 100°, and 130° as described in the text, the deduced logarithmic slopes $|S|$ of the angular correlations at $\pm 68°$ or $\pm 112°$ for Ge and NaI(Tl) detectors, and the resulting precessions (in mrad) $\Delta\theta(2^+_1\rightarrow 0^+_1)$ and $\Delta\theta(4^+_1\rightarrow 2^+_1)$. The errors in the slopes arise from the statistical errors determined in the measurement of the anisotropy ratios.

	^{78}Kr	^{80}Kr	^{82}Kr	^{84}Kr		^{86}Kr
Type of detector	Ge	Ge	NaI(Tl)	Ge	NaI(Tl)	NaI(Tl)
$\langle R\rangle(2^+_1)$	2.7(4)	2.8(2)	2.7(1)	3.0(1)	3.6(2)	2.9(2)
$\lvert S(2^+_1\rightarrow 0^+_1)\rvert$	2.21(13)	2.25(27)	2.27(6)	2.40(6)	2.86(14)	2.42(12)
$\lvert S(4^+_1\rightarrow 2^+_1)\rvert$	1.07(5)	0.94(9)	0.87(2)	1.05(4)	0.92(2)	-
$-\Delta\theta(2^+_1\rightarrow 0^+_1)$	25.1(16)	19.6(24)	20.1(7)	13.3(9)	13.0(9)	17.9(23)
$-\Delta\theta(4^+_1\rightarrow 2^+_1)$	21.9(33)	17.3(56)	8.9(62)	31.0(391)		

TABLE III. Comparison of the lifetimes (in ps) measured in this experiment with those listed in the literature.

Isotope		2_1^+	4_1^+	2_2^+
^{78}Kr	This work	27.5(25)	3.02(26)	
	Ref. [9]	34.5(19)	3.6(3)	5.34(58)
^{80}Kr	This work	11.32(72)	1.54(22)	
	Ref. [10]	12.67(7)	2.5(3)	11.0(20)
^{82}Kr	This work	6.69(20)		
	Ref. [11]	6.42(26)	0.97(36)	
^{84}Kr	This work	5.84(18)	0.95(18)	0.35(7)
	Ref. [12]	6.28(26)	$0.649(^{+72}_{-101})$	$0.433(^{+101}_{-43})$
^{86}Kr	This work	0.444(25)		
	Ref. [13]	0.318(26)	4473(865)	

B_m must be determined independently from Coulomb excitation calculations, to be verified via intensity measurements of the deexciting γ rays. For this case, the measured anisotropy ratio $\langle R\rangle$ is expressed as a weighted average of the feeding states,

$$\langle R(\theta_1/\theta_2)\rangle = \left(\frac{\sum_m P_m W_{m,i}(\theta_1) \sum_m P_m W_{m,j}(\theta_1)}{\sum_m P_m W_{m,i}(\theta_2) \sum_m P_m W_{m,j}(\theta_2)} \right)^{1/2}, \tag{3.4}$$

where, as before, the indices i and j refer to particular detectors. Each feeding transition has its own angular correlation function $W_m(\theta_\gamma)$:

$$W_m(\theta_\gamma) = 1 + \sum_k G_k Q_k A_{k,m}^{theo} P_k(\cos\theta_\gamma). \tag{3.5}$$

To a good approximation, G_k does not depend on m, hence the data can be analyzed with a single value of Q for all transitions. A single $\langle R\rangle$, measured for one state q is sufficient to determine the angular correlation coefficients for all other states. The measured average anisotropy ratios $\langle R\rangle$, logarithmic slopes and precessions $\Delta\theta$ are displayed in Table II.

The g factors were derived from the precession angles $\Delta\theta$, given by the expression

$$\Delta\theta = -g\frac{\mu_N}{\hbar}\int_{t_{in}}^{t_{out}} B[v(t),Z]e^{-t/\tau}dt, \tag{3.6}$$

where B, the transient field, was obtained using the Rutgers parametrization [6], t_{in} and t_{out} are the average times at which the excited ions enter or exit from the ferromagnetic foil, and τ is the meanlife of the state. In the absence of a nuclear state in a nucleus with the same atomic number and a g factor determined by an independent technique, a parametrization of the transient field needs to be used. The Rutgers parametrization was established from measurements of known g factors of states in nuclei ranging from O to Pt [6], and was used consistently in most measurements carried out with the transient field technique. While absolute g factors determined in this experiment depend on a parametrization of the transient field, the relative g factors do not, as they were obtained with the same target under the same kinematic conditions.

Most of the lifetimes relevant to the precessions of the corresponding nuclear states were redetermined by analyzing the Doppler-broadened line shapes of the emitted γ-ray lines. These were fitted for the known reaction kinematics applying stopping powers [15] to Monte Carlo simulations [19], including the second-order Doppler effect as well as the finite size and energy resolution of the Ge detectors at $\pm 112°$ and $\pm 68°$. The measured lifetimes and the deduced $B(E2)$'s are summarized in Tables III and IV. Significant differences between some of the present values and those quoted in the literature are found, and the lifetimes obtained from these measurements were used in the analysis of the g factors. In the present experiments on beams, the ions move with much higher velocities than available in the older experiments. Thus the analysis of the DSAM line shapes is less sensitive to systematic errors resulting from the uncertainty in the low-velocity stopping powers. In general, when the state lifetime is longer than the transit time through the ferromagnetic foil, the g factor is practically independent of the lifetime value. However, this condition does not apply to the 2_1^+ state of ^{86}Kr, where the extraction of the g factor from the precession data depends critically on the value of its lifetime. The best fit to the line shape of the ^{86}Kr$(2_1^+ \rightarrow 0_1^+)$ γ-ray transition is shown in Fig. 3. The resulting $g(I)$ are displayed in Fig. 4 and Table IV.

IV. DISCUSSION

The data indicate that the Kr isotopes are not monolithic but evolve through a variety of structures. The light ^{78,80,82}Kr

TABLE IV. Summary of g factors and $B(E2;2_1^+ \rightarrow 0_1^+)$'s in Weisskopf units. The g factors were determined by using the lifetimes measured in this experiment when available, and the literature data otherwise.

	^{78}Kr	^{80}Kr	^{82}Kr	^{84}Kr	^{86}Kr
$g(2_1^+)$	+0.43(3)	+0.38(5)	+0.40(2)	+0.27(1)	+1.12(14)
$g(4_1^+)$	+0.46(7)	+0.46(15)	+0.29(20)		
$g(2_2^+)$	+0.54(10)	+0.63(36)			
$B(E2;2_1^+ \rightarrow 0_1^+)$	76.9(70)	39.5(25)	20.4(6)	12.0(4)	8.7(5)
$B(E2;4_1^+ \rightarrow 2_1^+)$	105.4(91)	70.1(100)	32.1(119)	15.0(29)	0.05(1)
$B(E2;2_2^+ \rightarrow 2_1^+)$	5.9(6)	24.8(46)		13.0(2)	

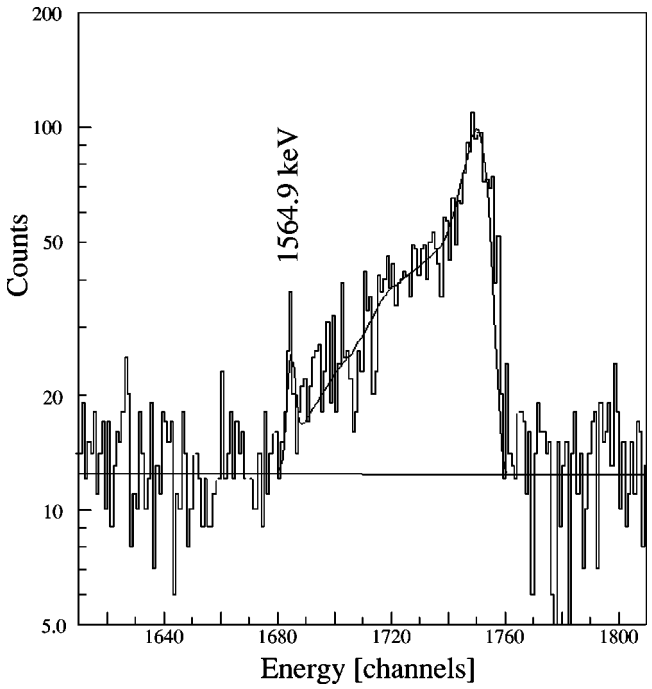

FIG. 3. DSAM line-shape analysis of the ^{86}Kr, $2_1^+ \rightarrow 0_1^+$, γ-ray transition, detected in the Ge detector at 0°. The sharp peak represents the stopped transition, and the broad structure on the right is reflective of the γ rays emitted in flight.

have large $B(E2)$'s indicating collectivity, albeit decreasing as the neutron occupation of the $g_{9/2}$ shell increases. The $g(2_1^+)$ values of these nuclei were calculated within the IBA-II model, with the parameters already successfully applied to the Se isotopes ($N_\pi = 3$) [5], but with $N_\pi = 4$. The neutron boson number N_ν is connected to N_π according to the constraint [20,22] $N_\pi \epsilon_{d_\pi} + N_\nu \epsilon_{d_\nu} = 0$, with ϵ_{d_π} and ϵ_{d_ν} being the single-particle energies of the proton and neutron bosons, respectively. It would be especially interesting to know whether a neutron shell closure at $N = 38$, as postulated for the Se isotopes, is also applicable to the Kr isotopes. Fits obtained with these parameters reproduce the g factors reasonably well, but completely miss the $B(E2)$'s. The best

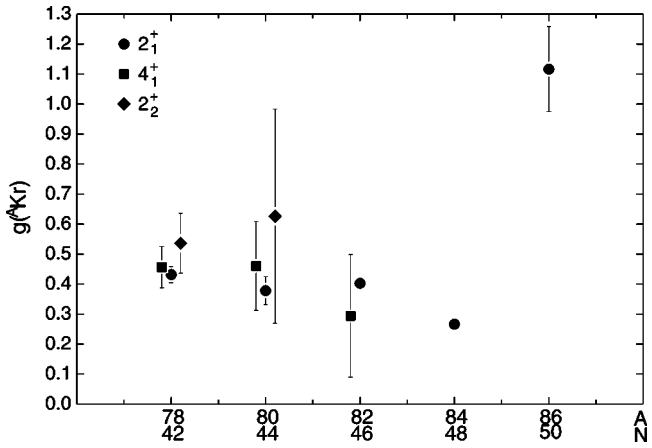

FIG. 4. Measured $g(I)$ factors of excited states in the ^{78,80,82,84,86}Kr isotopes.

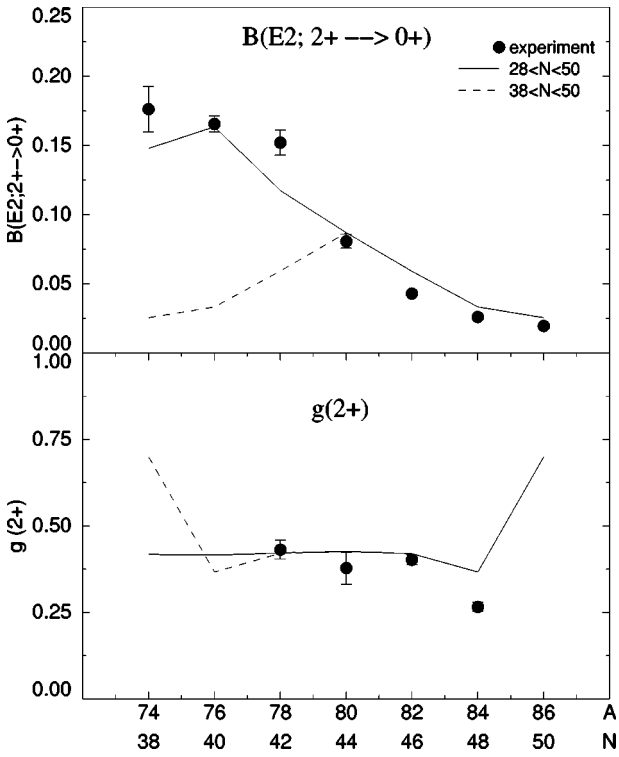

FIG. 5. Best fit of the g factors and $B(E2)$'s in units of e^2b^2 to IBA-II calculations.

simultaneous fits of both the g factors and the $B(E2)$'s in Kr were obtained by using the parameters listed in Table V and a shell closure at $N = 28$ (Fig. 5). The specific choice of the g_π and g_ν parameters follows from a semiempirical analysis of other g factors in this region, and are discussed in Refs. [20,21]. The energy levels of the low-lying levels of the Kr isotopes were actually best fit with a set of parameters that did not differentiate between proton and neutron bosons [23]. However, that calculation did not reproduce the $B(E2)$'s as well as the calculation with the parameters listed in Table V. Future measurements in the lighter, unstable ^{72,74,76}Kr isotopes might be a better indicator of shell closure at $N = 38$.

The g factor of the 2_1^+ state in $^{84}_{38}$Sr has also been explained within the framework of the IBA-II model [23], but without the need to invoke an effective boson number and

TABLE V. Summary of the parameters used for the $^{78-86}_{36}$Kr isotopes IBA-II study. The following parameters were used uniformly for all isotopes, $N_\pi = 4$, $\epsilon_d = 1.05$, $\epsilon_{d_\pi} = 0.075$, $\kappa = -0.13$, $\chi_\pi = \chi_\nu = -1.4$, $g_\pi = 0.7$, $g_\nu = 0.2$, and $e_\pi = e_\nu = 0.08\, e$b. The parameters representing the changes in neutron occupation are listed in the table.

A		78	80	82	84	86
$28 \leqslant N \leqslant 50$	N_ν	4	3	2	1	0
	ϵ_{d_ν}	−0.075	−0.10	−0.15	−0.30	0.0
$38 \leqslant N \leqslant 50$	N_ν	2	3	2	1	0
	ϵ_{d_ν}	−0.15	−0.10	−0.15	−0.30	0.0

TABLE VI. Comparison of $g(2_1^+)$ factors for Se (Ref. [5]), Kr and Sr (Ref. [3]) isotopes.

N	40	42	44	46	48	50
$_{34}$Se	+0.428(27)	+0.403(23)	+0.384(25)	+0.435(27)	+0.496(29)	—
$_{36}$Kr	—	+0.432(27)	+0.378(47)	+0.402(15)	+0.267(13)	+1.12(14)
$_{38}$Sr	—	—	—	+0.419(47)	+0.273(50)	+1.15(17)

subshell closure at either $Z=40$ or 38. Deformation in this nucleus has removed the $Z=40$ gap and proton bosons fill the 28–50 shell [3]. An additional IBA-II study involving parameters taken from Ref. [24] failed to reproduce the experimental data, assuming either a $N=28$ or 38 subshell closure.

At the other end of the shell, the large g factor of the 2_1^+ state of ^{86}Kr, with its closed neutron shell at $N=50$, clearly reflects proton configurations similar to those determining the g factors of the 2_1^+ states of the isotones ^{88}Sr, ^{90}Zr, and ^{92}Mo. It is noteworthy that the measured g factors of these nuclei, +1.15(17), +1.25(21) and +1.28(53), respectively, are within errors the same and are consistent with the value obtained for ^{86}Kr. A large shell model calculation [25], where ten protons and 22 neutrons can occupy the $f_{5/2}$, $p_{3/2}$, $p_{1/2}$, $g_{9/2}$, and $d_{5/2}$ orbits predicts $g(2_1^+)=1.34$ and $B(E2)=5.8$ W.u., in good agreement with the experimental values.

In ^{84}Kr, where two neutrons are removed from the $g_{9/2}$ orbit, the g factor shows a striking drop similar to what has been seen in ^{86}Sr. The g factor measured for ^{86}Sr, $g(2_1^+)=+0.274(50)$, is remarkably close to that of ^{84}Kr, where $g(2_1^+)=+0.267(13)$, again suggesting similar neutron and proton configurations in the wave functions of these nuclei. As the Schmidt value of $g_{9/2}$ neutrons is negative, $g_{\mathrm{Schmidt}}=-0.425$, the positive experimental value can only be obtained by including proton configurations as well, implying that the ^{86}Kr and ^{88}Sr cores are indeed not inert. The $g(2_1^+)$ factor of ^{86}Sr was successfully described as resulting from a configuration consisting of equal weights of two neutron holes in the $g_{9/2}$, $p_{1/2}$, $f_{5/2}$, and $p_{3/2}$ orbits coupled to the ground and first excited states of ^{88}Sr [26].

The close similarity of the nuclear wave functions of the Kr isotopes to neighboring Se and Sr isotopes is thus demonstrated by the experimental g factors of their 2_1^+ states (Table VI). This comparison suggests that supplementary data are desirable for the lighter isotopes ^{72}Se and ^{74,76}Kr, as well as ^{76,78,80,82}Sr. All these nuclei are unstable, but they could be studied if produced as radioactive beams with sufficient intensities. Recent measurements showed that difficulties arising from accumulation of radioactivity can be overcome, and that the present technique can therefore be applied to radioactive beams [27].

In summary, g factors of the low-lying states of the even Kr isotopes were obtained via projectile Coulomb excitation in inverse kinematics combined with the transient field technique. The data clearly show a transition from single-particle configurations at or near the $N=50$ shell closure (where neutrons and protons compete in the wave function) to more collective structures arising from the removal of neutrons from the $1g_{9/2}$ orbit. The signature of the neutron $1g_{9/2}$ shell is exhibited in the magnitude of the measured g factors. While the collective g factors are well described in the framework of the IBA-II model with the parameters listed in Table V, microscopic shell model calculations are needed for the two heavier isotopes ^{84,86}Kr. In view of the present systematics available on the stable Kr isotopes, an extension to the lighter unstable Kr isotopes ^{72,74,76}Kr is highly desirable. As the present technique is suitable for radioactive beams as well, this study will very likely be done when such beams become available.

ACKNOWLEDGMENTS

The authors are indebted to the staff of the Lawrence Berkeley National Laboratory 88 Inch Cyclotron for their assistance during the experiment. One of us (K.-H.S.) wishes to thank the Rutgers Nuclear Physics Laboratory for hosting summer visits during 1998–2000. The work was supported in part by the U.S. National Science Foundation, the BMBF, and the Deutsche Forschungsgemeinschaft. This work was also supported by the director, Office of Energy Research, Division of Nuclear Physics of the Office of High Energy and Nuclear Physics of the U.S. Department of Energy under Contract No. DE-AC03-76SF00098. J.H. acknowledges the support of a Sigma Xi Grant-in-Aid of Research. The authors are grateful to Professor Ani Aprahamian for the loan of two large Ge detectors, and for her interest in this work.

[1] A. L. Goodman, Phys. Rev. C **58**, R3051 (1998).
[2] S. Frauendorf and J. A. Sheikh, Nucl. Phys. **A645**, 509 (1999).
[3] A. I. Kucharska, J. Billowes, and M. A. Grace, J. Phys. G **14**, 65 (1988).
[4] G. Jakob, N. Benczer-Koller, J. Holden, G. Kumbartzki, T. J. Mertzimekis, K.-H. Speidel, C. W. Beausang, and R. Krücken, Phys. Lett. B **468**, 13 (1999); G. Jakob, N. Benczer-Koller, J. Holden, G. Kumbartzki, T. J. Mertzimekis, K.-H. Speidel, R. Ernst, P. Maier-Komor, C. W. Beausang, and R. Krücken, *ibid.* **494**, 187 (2000).
[5] K.-H. Speidel, N. Benczer-Koller, G. Kumbartzki, C. Barton, A. Gelberg, J. Holden, G. Jakob, N. Matt, R. H. Mayer, M. Satteson, R. Tanczyn, and L. Weissman, Phys. Rev. C **57**, 2181 (1998).
[6] N. K. B. Shu, D. Melnik, J. M. Brennan, W. Semmler, and N. Benczer-Koller, Phys. Rev. C **21**, 1828 (1980).

[7] J. Holden, N. Benczer-Koller, G. Jakob, G. Kumbartzki, T. J. Mertzimekis, K.-H. Speidel, A. Macchiavelli, M. McMahan, L. Phair, P. Maier-Komor, A. E. Stuchbery, W. F. Rogers, and A. D. Davies, Phys. Lett. B **493**, 7 (2000).
[8] J. Holden, N. Benczer-Koller, G. Jakob, G. Kumbartzki, T. J. Mertzimekis, K.-H. Speidel, A. Macchiavelli, M. McMahan, L. Phair, C. Beausang, R. Krücken, P. Maier-Komor, A. E. Stuchbery, W. F. Rogers, and A. D. Davies, Phys. Rev. C **63**, 024315 (2000).
[9] S. Rab, Nucl. Data Sheets **63**, 1 (1991).
[10] B. Singh, Nucl. Data Sheets **66**, 623 (1992).
[11] M. M. King and W.-T. Chou, Nucl. Data Sheets **76**, 285 (1995).
[12] J. K. Tuli, Nucl. Data Sheets **81**, 331 (1997).
[13] M. M. King, Nucl. Data Sheets **80**, 567 (1997).
[14] P. Maier-Komor, K.-H. Speidel, and A. Stolarz, Nucl. Instrum. Methods Phys. Res. A **334**, 191 (1993).
[15] F. J. Ziegler, J. Biersack and U. Littmark, *The Stopping and Range of Ions in Solids* (Pergamon, Oxford, 1985), Vol. 1.
[16] M. Hass, J. M. Brennan, H. T. King, T. K. Saylor, and R. Kalish, Phys. Rev. C **14**, 2119 (1976).
[17] R. Ernst, K.-H. Speidel, O. Kenn, A. Gohla, U. Nahum, J. Gerber, P. Maier-Komor, N. Benczer-Koller, G. Kumbartzki, G. Jakob, L. Zamick, and F. Nowacki, Phys. Rev. C **62**, 024305 (2000), and references therein.
[18] A. E. Stuchbery, I. Morrison, L. D. Wood, R. A. Bark, H. Yamada, and H. H. Bolotin, Nucl. Phys. **A435**, 635 (1985).
[19] J. C. Wells and N. R. Johnson, program LINESHAPE, 1994, ORNL.
[20] A. Wolf, *Perspectives for the Interacting Boson Model on the Occasion of its 20th Anniversary* (World Scientific, Singapore, 1994).
[21] A. Wolf, O. Scholten, and R. F. Casten, Phys. Lett. B **312**, 372 (1993).
[22] F. S. Radhi and N. M. Stewart, Z. Phys. A **356**, 145 (1996).
[23] U. Kaup, C. Mökemeyer, and P. von Brentano, Z. Phys. A **310**, 129 (1983).
[24] H. Dejbakhsh, A. Kolomiets, and S. Shlomo, Phys. Rev. C **51**, 573 (1995).
[25] E. K. Warburton, J. W. Olness, C. J. Lister, J. A. Becker, and S. D. Bloom, J. Phys. G **12**, 1017 (1986).
[26] C. A. Fields, F. W. N. de Boer, and J. Sau, Nucl. Phys. **A398**, 512 (1983).
[27] O. Kenn, K.-H. Speidel, R. Ernst, J. Gerber, P. Maier-Komor, N. Benczer-Koller, G. Kumbartzki, and F. Becker, Nucl. Instrum. Methods Phys. Res. B **171**, 589 (2000).